© 2019. Published by The Company of Biologists Ltd | Journal of Experimental Biology (2019) 222, jeb196659. doi:10.1242/jeb.196659

RESEARCH ARTICLE

Cutaneous respiration by diving beetles from underground aquifers of Western Australia (Coleoptera: Dytiscidae)

Karl K. Jones[1,*], Steven J. B. Cooper[1,2,3] and Roger S. Seymour[1]

ABSTRACT

Insects have a gas-filled respiratory system, which provides a challenge for those that have become aquatic secondarily. Diving beetles (Dytiscidae) use bubbles on the surface of their bodies to supply O_2 for their dives and passively gain O_2 from the water. However, these bubbles usually require replenishment at the water's surface. A highly diverse assemblage of subterranean dytiscids has evolved in isolated calcrete aquifers of Western Australia with limited/no access to an air–water interface, raising the question of how they are able to respire. We explored the hypothesis that they use cutaneous respiration by studying the mode of respiration in three subterranean dytiscid species from two isolated aquifers. The three beetle species consume O_2 directly from the water, but they lack structures on their bodies that could have respiratory function. They also have a lower metabolic rate than other insects. O_2 boundary layers surrounding the beetles are present, indicating that O_2 diffuses into the surface of their bodies via cutaneous respiration. Cuticle thickness measurements and other experimental results were incorporated into a mathematical model to understand whether cutaneous respiration limits beetle size. The model indicates that the cuticle contributes considerably to resistance in the O_2 cascade. As the beetles become larger, their metabolic scope narrows, potentially limiting their ability to allocate energy to mating, foraging and development at sizes above approximately 5 mg. However, the ability of these beetles to utilise cutaneous respiration has enabled the evolution of the largest assemblage of subterranean dytiscids in the world.

KEY WORDS: Allometry, Aquatic insect, Body mass, Boundary layer, Cuticle, Metabolic rate, Oxygen consumption

INTRODUCTION

Insects evolved in a terrestrial environment, as indicated by their gas-filled respiratory system (Pritchard et al., 1993). The tracheal system is a network of branching tubes that run from small openings (spiracles) on the outside of the insect's body through to the tissues to bring O_2 into close proximity with the mitochondria and allow CO_2 to move out. O_2 is able to diffuse through air 250,000 times faster than through water (Dejours, 1981) and, in combination with gas convection, the tracheal system of flying insects supplies the highest known mass-specific metabolic rate of any animal (Snelling et al., 2017). However, insect species in several groups, including Ephemeroptera, Plecoptera, Megaloptera, Trichoptera, Odonata, Diptera, Coleoptera and Hemiptera, have become aquatic secondarily, providing challenges for the gas-filled respiratory system (Foottit and Adler, 2009; Hutchinson, 1981).

Solutions to these challenges include air stores, which are bubbles taken underwater from which O_2 can be consumed during a dive, and gas gills, bubbles with a surface exposed to the water through which O_2 can diffuse, thus extending the dive. There are two types of gas gill: compressible and incompressible (plastrons). Compressible gas gills require replenishment at the surface as a result of both O_2 consumption by the insect and N_2 and CO_2 loss from the bubble to the water (Ege, 1915; Jones et al., 2015; Rahn and Paganelli, 1968; Seymour and Matthews, 2013). However, plastrons can be sustained indefinitely because of structures that prevent collapse of the bubble–water interface (Jones et al., 2018; Marx and Messner, 2012; Seymour and Matthews, 2013; Thorpe and Crisp, 1947a).

In addition to air stores and gas gills, many aquatic insects use cutaneous respiration. Some use tracheal gills, including mayfly, damselfly, stonefly and caddisfly larvae, and some small diving beetles with setal tracheal gills; in others, diffusion occurs through the unelaborated body surface, like the fifth instar of the aquatic bug *Aphelocheirus*, numerous dipteran larvae, and gill-less caddisfly and stonefly larvae (Bäumer et al., 2000; Eriksen, 1986; Kehl and Dettner, 2009; Morgan and O'Neil, 1931; Rasmussen, 1996; Thorpe and Crisp, 1947b; Verberk et al., 2018; Wichard and Komnick, 1974). Species that utilise cutaneous respiration contend with two significant types of resistance to diffusion in the O_2 cascade from the water to the tissues: the boundary layer (a water layer above a respiratory surface deficient in O_2 that provides resistance to diffusion) and the cuticle. In plastron breathers, the boundary layer can provide the greatest resistance in the O_2 cascade (Seymour et al., 2015). Consequently, plastron breathers are restricted to a small size, and have lower metabolic rates than insects in general, with *Aphelochirus* being the largest known species at 40 mg (Seymour and Matthews, 2013). This size limitation is associated with the relationship between metabolic rate, surface area and boundary layer thickness. The O_2 diffusion rate is, in part, affected by the quotient of surface area over boundary layer thickness, and as the insect becomes larger, the surface area relative to O_2 demand decreases, requiring the insects to have a thinner boundary layer to satisfy O_2 demand or a lower metabolic rate to avoid O_2 limitation, or both.

It is, therefore, anticipated that cutaneously respiring insects, without cuticular elaboration, would have lower metabolic rates and be smaller again than plastron breathers as a result of the additional resistance of the cuticle to O_2 diffusion. This hypothesis could be tested with subterranean aquatic beetles, as several pieces of evidence indicate that they use cutaneous respiration. Observations of two subterranean aquatic beetles indicate they lack plastrons,

[1]School of Biological Sciences, University of Adelaide, Adelaide, SA 5005, Australia. [2]Evolutionary Biology Unit, South Australian Museum, North Terrace, Adelaide, SA 5000, Australia. [3]Australian Centre for Evolutionary Biology and Biodiversity, University of Adelaide, Adelaide, SA 5005, Australia.

*Author for correspondence (karl.jones@adelaide.edu.au)

K.K.J., 0000-0002-0478-8021

Received 20 November 2018; Accepted 18 February 2019

Journal of Experimental Biology (2019) 222, jeb196659. doi:10.1242/jeb.196659

have little or no gas underneath the elytra to act as an air store and do not use gas gills (Ueno, 1957). However, subterranean aquatic beetles do have rich tracheation of the elytra and tolerate long periods of submergence, and are likely, as in some other subterranean species, to have low metabolic rates (Ordish, 1976; Smrž, 1981; Ueno, 1957). Additionally, the beetles may become trapped in interstitial spaces without air–water interfaces and would be unable to replenish their air stores (Ueno, 1957). Other than a small number of observations of these beetles' behaviour and habits (Ordish, 1976; Ueno, 1957), and quantification of the level of tracheation in the elytra of six subterranean diving beetles (Dytiscidae) (Smrž, 1981), no studies have thoroughly investigated respiration in subterranean aquatic beetles.

In Western Australia, there are more than 100 species of subterranean diving beetles described from approximately 50 isolated calcrete aquifers, representing the largest assemblage of subterranean diving beetles in the world (Balke et al., 2004; Watts and Humphreys, 2009). Each aquifer contains species of different size classes, but all species are less than 5 mm long (Balke et al., 2004; Watts and Humphreys, 2009). Most species (~75%) within each aquifer have evolved independently from separate surface-dwelling ancestors, with aridification of the Australian continent, after the Pliocene, likely to be the driver of their isolation in aquifers and evolution underground (Cooper et al., 2002; Guzik et al., 2009; Leys et al., 2003). However, there is also evidence that some species diversified underground from a subterranean ancestor (Cooper et al., 2002; Leijs et al., 2012; Leys and Watts, 2008; Leys et al., 2003). The aquifers are completely enclosed and it is likely that much of each aquifer does not have an air interface. The small size, lack of an air interface and apparent lack of setal tracheal gills found in some small surface dytiscids (Kehl, 2014) makes these diving beetles good candidates for cutaneous respiration.

In this study, we tested whether Australian subterranean dytiscids do use cutaneous respiration and investigated the hypothesis that cutaneous respiration limits them to a small size (<5 mm). We examined respiration in three subterranean dytiscids: *Paroster macrosturtensis* (Watts and Humphreys, 2006) and *Paroster mesosturtensis* (Watts and Humphreys, 2006), which are sympatric sister species from the Sturt Meadows calcrete aquifer; and an independently evolved species *Limbodessus palmulaoides* (Watts and Humphreys, 2006) from the Laverton Downs aquifer in Western Australia (Guzik et al., 2009, 2011; Watts and Humphreys, 2006). We tested whether their mode of respiration is similar to that of surface-dwelling species that use air stores and a small compressible gas gill (Calosi et al., 2007) and whether they use cutaneous respiration. We carried out closed-system respirometry to derive O_2-uptake measurements in all three species. In *P. macrosturtensis*, we determined the relationship between aquatic P_{O_2} and O_2 uptake. Fibre-optic O_2-sensing probes (optodes) were then used to measure O_2 boundary layers surrounding all three subterranean species, and scanning electron microscopy (SEM) showed they lacked structures such as pores or setae that could have respiratory significance. These results indicated that the beetles use cutaneous respiration. Cuticle thickness was measured in the subterranean species and six surface dytiscids to determine the relationship between cuticle thickness and size. The experimental data and measurements were then integrated into a respiration model based on Fick's general diffusion equation to assess conclusions made from experimental data and understand the limitations of cutaneous respiration on beetle size.

MATERIALS AND METHODS

Animals

Paroster macrosturtensis and *P. mesosturtensis* were collected during October 2015 and September 2016 from Sturt Meadows Station, and *L. palmulaoides* was collected during September 2016 from the Laverton Downs calcrete, WA. Beetles were captured with a 75 mm diameter plankton net attached to a fishing rod placed down boreholes into the calcrete aquifers (borehole depth 4.03–9.31 m, water depth 0.50–5.71 m at Sturt Meadows). After capture, beetles were placed in aquifer water in 200 ml plastic containers with some sand, small rocks and plant roots that were retrieved in the plankton net. The containers were maintained between 20 and 28°C and transported back to Adelaide by road before being placed in a constant temperature (CT) room at 24.5–25.5°C in darkness. Beetles were placed into plastic aquaria (22 cm L×13 cm W×14 cm H) with reverse osmosis (RO) water mixed with rock salt (Australian Sea Salt Rocks, Hoyts Food Industries P/L, Moorabbin, VIC, Australia) to a salinity of 19–22 ppt, and a ~5 mm layer of calcium carbonate sand and some calcrete stones were placed on the bottom of the aquaria. Water was lightly aerated with air pumped at 1–2 bubbles per second from a tube (4 mm i.d.). Beetles were fed 2–3 times a week with either small pieces of freshly killed amphipods (*Austrachiltonia australis*) or blackworm (*Lumbriculus* sp.). Beetles were weighed with an analytical balance (Mettler 163, Mettler, Greifensee, Switzerland; precision 0.01 mg) after each experiment or measurement.

Microscopy

Several species of small dytiscids have been identified as having structures such as setae or pores on the surfaces of their bodies that have, or may have, a respiratory function (Kehl and Dettner, 2009; Madsen, 2012; Verberk et al., 2018). To determine whether these structures were present on the subterranean species, we used SEM. Specimens that had been kept in 100% ethanol were air dried, mounted on stubs, sputter coated with platinum, and viewed with a scanning electron microscope (Quanta 450, FEI, Tokyo, Japan).

To understand how the structure of the cuticle relates to O_2 diffusion, we histologically examined thin sections of the cuticle. For sectioning of the ventral and elytral cuticle, the heads of beetles were removed and the abdomens were then placed in electron microscopy fixative (4% paraformaldehyde/1.25% glutaraldehyde in PBS, +4% sucrose, pH 7.2) for at least 24 h. Samples were then washed in buffer (PBS+4% sucrose, 10 min), post-fixed with 2% OsO_4 for 1 h, and passed through an ethanol series (2×70%, 2×90%, 3×100%, 15 min each), then propylene oxide (15 min), a 1:1 mixture of propylene oxide and epoxy resin for ~3 h, then two changes of 100% resin for ~5.5 and 16 h, before being placed in fresh resin and polymerized at 70°C for at least 24 h. Sections, 1–2 µm thick, were made through the transverse plane midway along the abdomen using a microtome (Leica EM UC6, Leica Mikrosysteme GmbH, Vienna, Austria), and samples were stained with a 1% Toluidine Blue and 1% borax mixture. Although samples were prepared for transmission electron microscopy, they were viewed under a light microscope. Four cuticle thickness measurements from each sample produced a mean value for that sample. Some beetle specimens had been prepared and stored differently prior to fixation, including freshly killed specimens, those stored in 70% and 100% ethanol, and air-dried specimens. Data were pooled for each species for comparisons among species.

Cuticle samples from freshly killed surface species were also taken and prepared in the same manner as above to produce an allometric relationship of cuticle thickness with mass. Species

included were *Necterosoma dispar* (Germar 1848), *Rhantus suturalis* (W. S. Macleay 1825), *Sternopriscus clavatus* Sharp 1882, *Platynectes decempunctatus* (Fabricius 1775), *Onychohydrus scutellaris* (Germar 1848) and *Hyderodes shuckardi* Hope 1838 (Watts and Hamom, 2014). *Necterosoma dispar*, *R. suturalis* and *S. clavatus* were collected near Forreston in the Adelaide Hills, SA, *P. decempunctatus* from near Strathalbyn, SA, and *O. scutellaris* and *H. shuckardi* from near Penola, SA, between February and May 2017. For larger surface species, cuticular samples were taken from the centre of an elytron and abdominal sternite 4, and in smaller species from the centre third of an elytron and sternites 2–4.

The simple structure of the ventral cuticle formed by a number of parallel laminae contrasts with the elytral cuticle. The elytral cuticle in small species consists of a layer of parallel laminae with a layer of soft tissue on the ventral surface. However, in larger species, from *P. decempunctatus* (28 mg) up, there are haemolymph spaces that are encompassed within the cuticular laminae to varying degrees (Noh et al., 2016). Cuticle thickness was measured on the ventral surface perpendicular to the cuticular laminae from the outside surface through to the soft tissue, and in the elytra from the outside surface including, or excluding, the soft tissue or haemolymph spaces.

Boundary layer thickness

If O_2 is taken up from the water through a surface such as the cuticle or a gas gill bubble, O_2 diffusion will be evident by a decrease in P_{O_2} from the free water through a layer next to that surface, called the boundary layer, and the effective thickness can be measured by the distance from the beginning of the P_{O_2} decrease to the surface. Boundary layer thickness in the subterranean dytiscids was detected and measured with a fast-response fibre-optic O_2-sensing optode (Sensor model, PSt 1 taper tip, tip diameter <50 µm; meter model TX-3; PreSens, Regensburg, Germany) mounted in a 3D micromanipulator (Seymour et al., 2015). Individuals of the three subterranean species were glued with cyanomethacrylate gel either dorsally or ventrally to a small wire stand that was placed into a clear Perspex container (110 mm L×90 mm W×25 mm H) with 15 mm-deep stagnant water. If placed with the ventral surface upwards, a small amount of glue was used to restrain the legs as movement would disrupt the boundary layer and P_{O_2} measurements. A dissecting microscope was mounted horizontal and perpendicular to the Perspex container to view the beetle ∼1 cm below the surface. The optode was lowered to the surface of the beetle and progressively raised in 50 µm steps until 200 µm above the surface of the beetle, then in 100 µm steps to 500 µm, and 250 µm steps to 1000 µm. The optode was left for measurements at each position for 30 s, after which a 30 s recording period took place before the optode was moved to the next measurement position. Optodes were calibrated weekly with sodium sulphite and air-equilibrated water at the measurement temperature. In a pilot study, we attempted to detect boundary layers above the cuticle of the large surface dytiscid *O. scutellaris*. However, no P_{O_2} differences consistent with the presence of a boundary layer were detected on the elytron, metacoxa, metafemur or sternites. This pilot study provided evidence that optode measurements in the subterranean beetles were unlikely to be caused by changes in sensor readings when approaching the surfaces of the beetles, or by microbial growth.

Respirometry

Two methods of respirometry were used to measure O_2 consumption rate in the beetles. The first involved a closed chamber with water and a small amount of air in which P_{O_2} was measured with an optode (Sensor model, B2 flat tip; PreSens). Only the O_2 consumption of *P. macrosturtensis* was measured with this method when it was unknown whether the beetles returned to the surface to collect air. Once it was established that the beetles could remain underwater for long periods, a second method was used involving a closed respirometry chamber, filled with water only, where P_{O_2} was measured with a Clark-type O_2 electrode. This chamber was subsequently used for *P. macrosturtensis*, *P. mesosturtensis* and *L. palmulaoides*.

The first setup consisted of a glass vial, 41 mm long, 18 mm in diameter with a 7 mm diameter opening. Nylon mesh surrounded the inner sides and bottom of the jar to prevent beetles getting stuck to the glass and allow them to get to the surface if needed. The jar was filled with air-equilibrated RO water with dissolved NaCl at 25°C and 22 ppt salinity. Individual beetles were placed into the chambers in a drop of water, minimising the introduction of bacteria and preventing the beetle from getting stuck on the meniscus. Chambers were then sealed with a chemical stopper, with excess water pushed through a 1 mm hole in the stopper. The chamber was then dried on the outside and weighed with the analytical balance. Afterwards, approximately 0.2 ml of water-saturated air at 25°C was injected into the chamber, pushing excess water out. The chamber was dried and weighed again. A water-filled Pasteur pipette was then inserted into the chamber, through the hole in the stopper. The chamber was then placed into a water bath regulated by a thermocirculator (Thermomix 1419, type 850094, B. Braun, Melsungen, Germany), and left for 4–5 min to allow the temperature to equilibrate. An optode was inserted through the tight-fitting pipette to measure P_{O_2}, effectively sealing the chamber with water. The optode inserted into the bubble, and then water, recorded the initial P_{O_2} in each medium for 2 min after the P_{O_2} traces became stable (∼2–4 min). Each chamber was left for approximately 3 h, after which the optode was placed back into the air bubble, and then the water, which was gently mixed producing a uniform distribution of O_2 for final P_{O_2} measurements (2 min stable trace). The beetle was then removed from the chamber, dried with a paper towel and weighed live. The experimental water was returned to the chamber, which was topped up with fresh RO water and closed. The pipette and optode were inserted into the chamber, which was returned to the water bath. The water-filled chambers were used to assess background respiration and sensor drift and left for approximately 3 h between initial and final P_{O_2} measurements. If background respiration and drift exceeded ±10% O_2 uptake, data were excluded. Air and water volumes in the chambers were determined from the mass measurements of the chambers with water, and air and water minus beetle wet mass (if present), and the dry mass of the chambers, the chemical stopper seal and mesh.

The second respirometry setup, used while at Sturt Meadows Station, consisted of four closed water-filled high-density polyethylene chambers with a glass front (0.67 ml, model 1271, Diamond General, Ann Arbor, MI, USA), each with a Clark-type O_2-electrode (model 730, Micro-electrodes, Bedford, NH, USA) (Mueller and Seymour, 2011). Temperature was regulated by circulating water at the experimental temperature through a water bath and water jackets surrounding the respiratory chambers. The electrodes were connected to an O_2-analyser (ReadOx-4H, Sable Systems, Las Vegas, NV, USA), a data acquisition unit (PowerLab ML750, ADInstruments Pty Ltd, Castle Hill, NSW, Australia) and a laptop computer, and were calibrated with sodium sulphite every 1–4 days (zero drifted ≤1% per day) and air-equilibrated water daily. In the back of each chamber was a miniature magnetic stirrer that rotated at ∼2 Hz.

For air-equilibrated $\dot{M}_{O_2}$ measurements, chambers were 2/3 filled with water and the stable P_{O_2} recorded for 5 min, providing an initial

measurement for drift calculation. Drift was assumed to be linear (Seymour and Roberts, 1995). Individual *P. macrosturtensis* or *L. palmulaoides*, or four *P. mesosturtensis* because of their small size, were then pipetted into the open chambers, which were closed and filled with the treatment water, ensuring no air bubbles remained. Beetles were left for approximately 2 h with the stirrer on to maintain homogeneous P_{O_2} before the beetles were removed and the experimental water put aside. Chambers were again 2/3 filled with air-equilibrated water for a second stable 5 min period to calculate drift over the time beetles were in the chambers. The water that contained the beetles was then returned to the chamber for 30 min to measure background respiration, followed by another stable 5 min period with clean water for drift calculation during background respiration measurement.

Water saturation in boreholes where beetles are found can vary widely both between and within boreholes (Fig. S1). Because of this variation, the relationship between O_2 consumption rate and declining P_{O_2} was measured in *P. macrosturtensis* to understand how these conditions might affect metabolism. Individual *P. macrosturtensis* were exposed to four individual P_{O_2} treatments in the 0.67 ml chambers, nominally ∼20, ∼15, ∼10 and ∼5 kPa. This was done to avoid excessive build-up of CO_2 and bacterial contamination that would have occurred in one long respirometry run. Beetles were placed into the chambers for 1.5 h, then removed and background respiration measured for 30 min. Prior to and after each measurement, 5 min periods of P_{O_2} were measured as above for drift determination.

$\dot{M}_{O_2}$ was calculated in both respirometry methods with Eqn 1:

$$\dot{M}_{O_2} = \beta_{O_2} \times V \times \dot{P}_{O_2}, \quad (1)$$

where $\dot{M}_{O_2}$ (μmol h^{-1}) is the rate of O_2 consumption, β_{O_2} is the capacitance of the medium for O_2 (μmol ml^{-1} kPa^{-1}), V is the volume of the medium (ml) and $\dot{P}_{O_2}$ is the rate of decrease of P_{O_2} in the medium (kPa h^{-1}). β_{O_2} at 25°C in the air was 0.4032, and in the water, accounting for salinity, it was 0.01130 at 19 ppt, 0.01117 at 21 ppt and 0.01110 at 22 ppt, assuming a linear change in capacitance from 0 to 35 ppt salinity (Dejours, 1981). V of water was ∼6 ml and that of air was ∼0.19 ml in the air+water chambers, and 0.67 ml in the water-only chambers. $\dot{P}_{O_2}$ decline in the air+water chambers was determined from the initial and final P_{O_2} measurements and time between them, and to calculate total $\dot{M}_{O_2}$, $\dot{M}_{O_2}$ in each medium was summed. $\dot{P}_{O_2}$ in water-only chambers was determined directly from the linear slope of the P_{O_2} trace.

The rate of P_{O_2} decline (or $\dot{M}_{O_2}$ decline in the air+water chambers) of the background measurement was subtracted from the total respiration rate of the chamber with the beetle in it to determine the beetles' $\dot{M}_{O_2}$. Background respiration was 4.1±3.1% of the total (N=7) in the air+water chambers with *P. macrosturtensis*, and 6.4±4.4% (N=7) in the water-only chambers, and 20.1±7.1% (N=27) for the critical P_{O_2} measurements. For *P. mesosturtensis*, background respiration was 29.6±24.5% (N=5), and for *L. palmulaoides* it was 40.7±20.6% (N=6).

Activity of the beetles, e.g. crawling or moving legs or body, was assessed in beetles within the water-filled respirometry chambers as the cumulative duration of activity of one or more beetles within the chamber over a 10 min period. A stopwatch was used while observing the beetles and activity was reported as the percentage of time active during the 10 min period.

Wet mass of *P. macrosturtensis* was recorded from air+water chamber experiments conducted in the lab; however, all other experiments took place at the field station at Sturt Meadows, where a balance was unavailable. There, beetles were dried with silica gel beads and weighed with the analytical balance once back in the lab. Wet mass was reconstructed from dry mass using the water content of living beetles, which was found to be 66.5% of wet mass.

The subterranean beetles hold a small amount of gas within the sub-elytral cavity but are slightly negatively buoyant. The O_2 within this gas was not included in calculations of $\dot{M}_{O_2}$ because it represents only 1% of the O_2 in the water-only chambers and <0.1% in the air+water chambers.

Field measurements: video recording of beetles in boreholes

Video recording of the beetles in the boreholes was undertaken to quantify the beetles' activity and pattern of occurrence, which may be related to O_2 levels or resource availability within the boreholes. To record the beetle's activity, we mounted a bore camera (USB Endoscope Camera, 20 m, 14.5 mm diameter, with four LEDs), angled at ∼45 deg downward on a weight on the end of a tape measure. The camera was orientated so the view was not obstructed by the side of the borehole, and was placed at the water surface, at 0.5 m depth and at the bottom of each hole (N=11 boreholes surveyed). Water depth at the bottom varied between holes. The three beetle species found at Sturt Meadows – *P. macrosturtensis*, *P. mesosturtensis* and *P. microsturtensis* – were not distinguished in the video recordings as parallax and distortion made it difficult to discern size and shape differences between species. Recordings at each point within the borehole were made for 600 s and observed using a VLC media player (version 2.2.3, USA). The number of occurrences of beetles was counted. An occurrence counted as a beetle entering the camera view. The proportion of time beetles were active in boreholes was determined by measuring how long beetles were in view of the camera and recording when and how often beetles were active.

Statistics

Wilcoxon matched pairs, ANOVA and Tukey's *post hoc* tests were conducted with GraphPad Prism 7.02 (GraphPad Software Inc., La Jolla, CA, USA), and ANCOVA were conducted according to Zar, 1998. Linear, one-phase association, power and polynomial regressions were performed with Excel or GraphPad Prism. Statistics reported are means and 95% confidence intervals.

RESULTS

Microscopy

The dorsal surfaces of the head, pronotum and elytra of *P. macrosturtensis* and *P. mesosturtensis* were very similar (Fig. 1A,B). Both species had very sparse setae with the dominant structures being hexagonal reticulations on all three surfaces viewed. *Limbodessus palmulaoides* also had sparse setae, but the pronotum and elytra were smooth with no visible reticulations, and the head showed irregular hexagonal reticulations (Fig. 1C). The ventral surface of *P. macrosturtensis* was also viewed and was similar to the dorsal surface.

Cuticle structure and thickness

Cuticle structure varied between dorsal and ventral surfaces, as well as between the elytral cuticles of different species. The ventral cuticle consisted of a number of parallel cuticular laminae next to the soft tissue of the abdomen in all species (Fig. 2E,F). However, the elytral cuticle in the small dytiscids (subterranean species, and *S. clavatus* and *N. dispar*) consisted of a layer of parallel laminae with a thin layer of soft tissue on the ventral surface of the elytra (Fig. 2D). Tracheae were visible within the soft tissue, which in the

Journal of Experimental Biology (2019) 222, jeb196659. doi:10.1242/jeb.196659

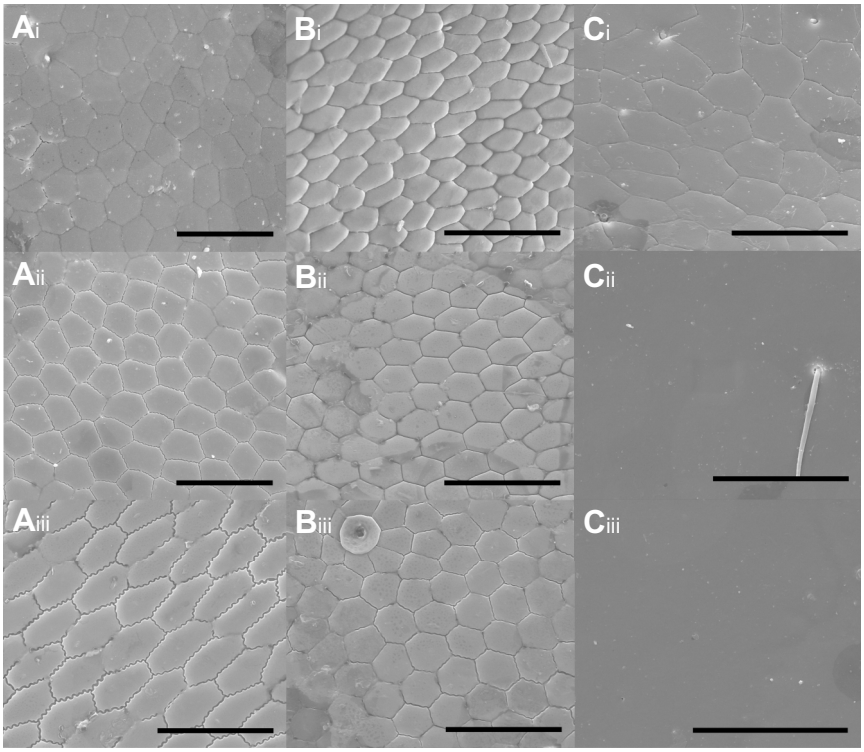

Fig. 1. Scanning electron microscopy (SEM) images of the three subterranean beetle species. *Paroster macrosturtensis* (A), *Paroster mesosturtensis* (B) and *Limbodessus palmulaoides* (C), showing dorsal surfaces of the head (i), pronotum (ii) and elytron (iii). Scale bars: 20 µm.

sections were small circular structures that correspond with the tracheae seen in the elytra of living beetles. In the larger species (*O. scutellaris*, *H. shuckardi*, *P. decempunctatus* and *R. suturalis*), haemolymph spaces were seen between a dorsal and ventral layer of cuticular laminae separated by trabeculae, pillar-like structures consisting of the chitinous laminae, except in *P. decempunctatus*, where they were absent or poorly developed (Fig. 2A–C; Noh et al., 2016; Van de Kamp and Greven, 2010). Observations of beetle elytra in another study suggest the tracheae are within the haemolymph spaces (Iwamoto et al., 2002).

The cuticle thickness of all surface dytiscids was significantly greater than that in the subterranean species (Table 1, Fig. 3). The dorsal and ventral thickness data were pooled to produce an allometric regression of cuticle thickness. Dorsal measurements that excluded the soft tissue and haemolymph spaces were used. These values were the most relevant to O_2 diffusion through the cuticle because of the presence of tracheae within the soft tissue and probably within the haemolymph spaces. The pooled data of both surface and subterranean species showed that cuticle thickness increased with mass to the exponent 0.31±0.05 (Fig. 3).These data were not phylogenetically corrected because of the small number of taxa used in the analysis. The ability to detect phylogenetic signal in a trait is much lower where analyses have fewer than 20 taxa (Blomberg et al., 2003). Additionally, a phylogenetically corrected regression may differ from the observed regression, which would result in diffusion models based on the corrected data being less representative of the actual system.

O_2 boundary layers

O_2 boundary layers were found on both the dorsal and ventral surfaces of *P. macrosturtensis*, *P. mesosturtensis* and *L. palmulaoides* (Fig. 4A). To reduce variation associated with small differences in the P_{O_2} of the water in which the beetles were placed, the difference (ΔP_{O_2}) between the maximum P_{O_2} value recorded in each P_{O_2} trace and the P_{O_2} value at each measurement position was calculated (Fig. 4B). To approximate the effective boundary layer thickness, a one-phase association was applied to the ΔP_{O_2} data (Fig. 4B) where $\Delta P_{O_2}=Y_0+(\text{Plateau}-Y_0)\times(1-\exp^{(-k\times X)})$, where Y_0 is the y-intercept, and the plateau was constrained to 0 representing the P_{O_2} of the surrounding water. The effective boundary layer thickness was defined as where the ΔP_{O_2} (Y) is 5% different from zero where Y_0 equals 100%. The boundary layer thickness (X) was calculated by rearranging the one-phase association, where $X=[\ln(Y/Y_0)]/-k$ (excluding the plateau which equals 0; Fig. 4B). For *P. macrosturtensis*, $Y_0=-4.995$ and $k=0.004363$ (dorsal, $R^2=0.80$), and $Y_0=-7.576$ and $k=0.003739$ (ventral, $R^2=0.88$), for *L. palmulaoides*, $Y_0=-9.067$ and $k=0.004175$ (dorsal, $R^2=0.88$), and $Y_0=-7.222$ and $k=0.004689$ (ventral, $R^2=0.92$), and for *P. mesosturtensis* $Y_0=-5.312$ and $k=0.006659$ (dorsal, $R^2=0.73$), and $Y_0=-4.113$ and $k=0.006561$ (ventral, $R^2=0.81$). In *P. macrosturtensis*, the dorsal and ventral boundary layers were 687 µm and 801 µm, respectively; in *L. palmulaoides*, the dorsal and ventral boundary layers were 718 µm and 639 µm, respectively; and in *P. mesosturtensis*, the dorsal and ventral boundary layers were 450 µm and 457 µm, respectively. The P_{O_2} within the boundary layer of *P. macrosturtensis* on the ventral surface was significantly lower than that within the layer at the dorsal surface at distances less than 400 µm from the surface of the beetles (two-way ANOVA, $P<0.0001$, Tukey's *post hoc*, $P\leq0.01$). In *L. palmulaoides*, the P_{O_2} within the ventral boundary layer was significantly higher than that for the dorsal surface from 200 µm to the surface (Tukey's *post hoc*, $P\leq0.01$). In *P. mesosturtensis*, there are no differences between the dorsal and ventral boundary layers until at the surface where the ventral P_{O_2} was significantly higher than the dorsal P_{O_2} (Tukey's *post hoc*, $P\leq0.01$).

Respirometry

Mass-specific $\dot{M}_{O_2}$ was not significantly different between all three subterranean species in the water-only chambers (Table 2; ANOVA). However, *P. macrosturtensis* in the air+water chambers had a

Journal of Experimental Biology (2019) 222, jeb196659. doi:10.1242/jeb.196659

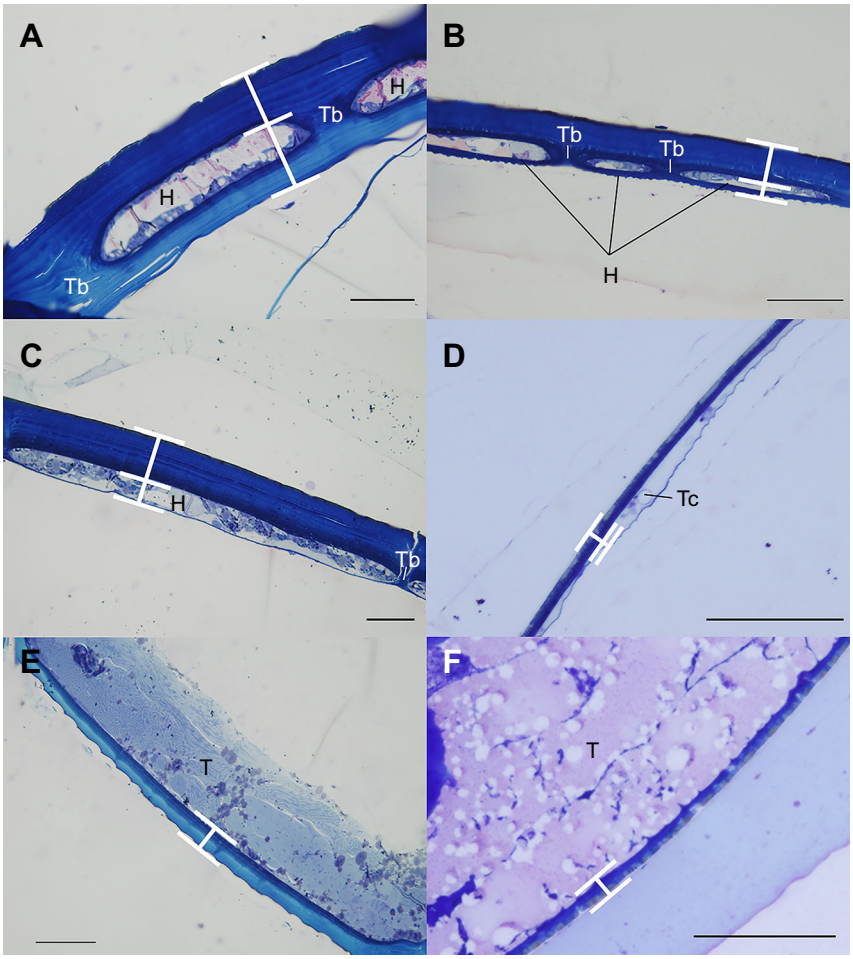

Fig. 2. Cuticle structure and thickness. Sections of dytiscid cuticle showing differing levels of integration of the haemolymph spaces (H) and trabeculae (Tb) in the elytra of large dytiscids (above ~25 mg) and the trachea (Tc) in the soft tissue of small dytiscids (below ~10 mg), and the simple ventral cuticle with soft tissue (T) on the dorsal side. (A–D) Elytra, with the dorsal surface orientated towards the top of the figure. (E,F) Ventral cuticle, with the ventral surface orientated towards the bottom of figure. White bars show examples of how cuticle thickness was measured in the different species by measuring the perpendicular distance between the surfaces of the cuticle. A: *Onychohydrus scutellaris*; B: *Rhantus suturalis*; C: *Hyderodes shuckardi*; D: *P. macrosturtensis*; E: *Sternopriscus clavatus*; F, *P. macrosturtensis*. Scale bars: 100 µm.

significantly higher mass-specific metabolic rate than *L. palmulaoides* (Table 2; ANOVA, $P<0.05$, Tukey's *post hoc*). Whole-animal $\dot{M}_{O_2}$ was significantly different between all species and experimental setups except for *L. palmulaoides* and *P. macrosturtensis* in the water-only chambers (Table 2; ANOVA, $P<0.0001$, Tukey's *post hoc*). Mean percentage of time that individual beetles were active in the water-only chambers over a 10 min period was 15% in *P. macrosturtensis* (N=8) and 3% in *L. palmulaoides* (N=6). Mean percentage of time that one or more beetles were active with *P. mesosturtensis* within the chambers was 1% (N=2). On occasion, beetles clung to the magnetic flea in the chamber; however, while not moving, these beetles may not have had a resting metabolism.

As *P. macrosturtensis* was exposed to progressively lower P_{O_2}, $\dot{M}_{O_2}$ declined, as indicated by a linear regression (solid orange line in Fig. 5), and a decline in the upper bounds of $\dot{M}_{O_2}$ measured at a given P_{O_2} (dashed black line, N=11 beetles, dry mass 1.08±0.13 mg, calculated wet mass 3.23±0.4 mg).

Table 1. Mass of dytiscids, and dorsal and ventral cuticle thickness

		Dorsal (µm)		
Species	Mass (mg)	Excluding H/ST	Including H/ST	Ventral (µm)
P. mesosturtensis	0.55*	**7.2±0.3 (7)**	11.1±0.5 (7)	**8.4±0.7 (6)**
L. palmulaoides	2.32*	**6.4±0.7 (8)**	12.2±2.1 (6)	**6.5±0.5 (7)**
P. macrosturtensis	2.72*	**7.5±0.5 (13)**	12.2±2.4 (12)	**7.7±0.7 (11)**
S. clavatus	3.95±0.46 (8)	**42.9±3.6 (8)**	51.0±2.8 (7)	**33.0±2.4 (7)**
N. dispar	7.7±0.5 (6)	**43.0±4.0 (6)**	50.2±3.5 (6)	**38.6±5.2 (6)**
P. decempunctatus	28.54±2.24 (8)	**35.0±3.7 (8)**	44.6±5.2 (8)	**32.9±2.4 (8)**
R. suturalis	101.11±8.38 (8)	**34.8±3.1 (8)**	60.8±4.1 (8)	**34.7±3.4 (8)**
H. shuckardi	627.45±37.79 (8)	**76.9±6.9 (8)**	119.0±6.7 (8)	**70.7±7.4 (8)**
O. scutellaris	1319.42±119.77 (8)	**67.3±7.0 (7.0)**	171.2±19.3 (8)	**103.6±23.3 (8)**

Data are for *Paroster mesosturtensis*, *Limbodessus palmulaoides*, *Paroster macrosturtensis*, *Sternopriscus clavatus*, *Necterosoma dispar*, *Platynectes decempunctatus*, *Rhantus suturalis*, *Hyderodes shuckardi* and *Onychohydrus scutellaris*. Dorsal (elytral) data are split into those excluding and including haemolymph spaces and soft tissue (H/ST). Means and 95% CIs are shown with *N* in parentheses.
*Wet mass values calculated from dry mass. Bold values were used for cuticle thickness regression in Fig. 3. The thickness of the cuticle including the soft tissue in subterranean species may be artificially reduced because of some samples being dried or stored in ethanol before fixation.

Journal of Experimental Biology (2019) 222, jeb196659. doi:10.1242/jeb.196659

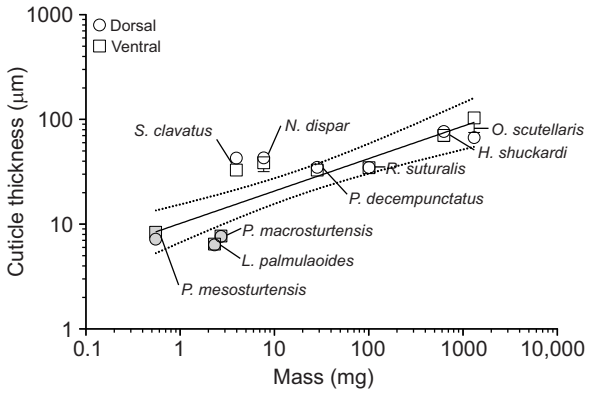

Fig. 3. Allometric regression of dorsal cuticle thickness, excluding the haemolymph spaces and soft tissue, and ventral cuticle thickness of dytiscids. Subterranean species are indicated by grey symbols. Values are means with 95% confidence intervals (CIs). Many error bars are shorter than the symbols and are therefore not visible. Cuticle thickness=$10.162M_b^{0.31}$ (where M_b is body mass), regression showing 95% CI bands.

Field measurements

Eight of 11 boreholes surveyed with the borescope contained beetles. Water depth in the boreholes with beetles was 2.7±1.7 m (range 0.50–5.71 m). The mean number of beetle occurrences over 10 min was 4.8±4.4 (N=8) at the surface, 1.7±1.1 (N=6) at 50 cm water depth, and 2.1±2.4 (N=8) at the bottom of the boreholes. Two boreholes had total depths of 0.50 and 0.65 m and these records are included in the bottom category. The number of beetle occurrences at the surface was significantly higher than at the bottom (Wilcoxon matched pairs non-parametric test, P<0.05). The mean percentage of time individual beetles spent active while in the view of the camera, either swimming or crawling in boreholes, was 71±7% (N=50 observations determined from six boreholes), spending an average of 9.9±7.8 s in the view of the camera with 3.08 bouts of activity during this time.

DISCUSSION

Cutaneous respiration in subterranean dytiscids

This study shows that small subterranean diving beetles rely entirely on cutaneous respiration, in which O_2 diffuses from the water through the O_2 boundary layer to the beetles' surface and then through the cuticular laminae. On the ventral surface, O_2 diffuses directly into the tissues, but on the dorsal surface of the elytra, it goes into the thin layer of soft tissue or the tracheoles within that tissue, as well as the sub-elytral cavity. In all three species, the sub-elytral cavity is gas filled, so O_2 entering this space could diffuse to the spiracles on the dorsal side of the abdomen and into the tracheal system or diffuse directly through the tergites. SEM showed the tergites are not hardened like the elytra or sternites.

Unlike in surface-dwelling dytiscids, the gas within the sub-elytral cavity does not appear to be exchanged with the air or water directly. These beetles rarely go to the surface and break the meniscus with the tip of the abdomen, and were never observed to have a small gas gill bubble at the tip of the abdomen, like in surface species. Additionally, *P. macrosturtensis* and *P. mesosturtensis* have tightly locked elytra (Watts and Humphreys, 2006). Consistent with the hypothesis that the beetles use cutaneous respiration, we observed the beetles could survive at least 12 days submergence without access to air, and they are slightly negatively buoyant. Another subterranean beetle, *Phreatodytes relictus* (Noteridae), lacks gas under the elytra completely (Ueno, 1957), showing that respiratory involvement of this space is not necessary.

The strongest support for cutaneous respiration in *P. macrosturtensis*, *P. mesosturtensis* and *L. palmulaoides* is the presence of O_2 boundary layers surrounding the beetles, indicating O_2 diffusion into the surface of their bodies (Fig. 4). Boundary layer thickness on the dorsal surface is similar to that on the ventral surface in *P. mesosturtensis*, 450 and 457 μm, respectively. However, in *P. macrosturtensis* and *L. palmulaoides*, the dorsal layers (687 and 718 μm, respectively) differ from the ventral layers (801 and 639 μm, respectively; Fig. 4). The difference in thickness between the dorsal and ventral boundary layers is unclear, but may be linked to differences in the cuticle thickness more widely across the body despite the similarities measured in thin sections. The thinner boundary layer found around *P. mesosturtensis* is due to this species' smaller size. In experiments, glue holding the beetles to the stand would increase O_2 demand through the other surfaces that are not covered, thus increasing the boundary layer thickness. Under natural conditions, the boundary layers are likely to be thinner, because the beetles are often moving (mean 3.08 bouts of activity over an average of 9.9 s while in view of the borescope), and, at least at Sturt Meadows, there appears to be some slow water movement within the aquifer that would help ventilate the boundary layer.

Modelling external diffusion barriers

Fick's general diffusion equation (Eqn 2) can be used to model diffusion from the water to a respiratory surface, such as a gas gill (Rahn and Paganelli, 1968):

$$\dot{M}_{O_2} = K_{O_2} \times A/X \times \Delta P_{O_2}, \quad (2)$$

where $\dot{M}_{O_2}$ (pmol s^{-1}) is the rate of O_2 consumption, K_{O_2} (pmol s^{-1} kPa^{-1} cm^{-1}) is Krogh's coefficient of diffusion, the product of capacitance and diffusivity, A (cm^2) is the surface area for gas exchange, X (cm) is the thickness of the boundary layer and ΔP_{O_2} (kPa) is the P_{O_2} difference between the surrounding water and respiratory surface. This equation can be rearranged to calculate P_{O_2} through the O_2 cascade of the subterranean beetles to evaluate the extent of diffusion limitations to respiration (Table S1). P_{O_2} at the surface of the beetles and on the inside of the cuticle, representing O_2 diffusion through the boundary layer and then through the cuticle, can be calculated with the experimentally determined $\dot{M}_{O_2}$, under different convective conditions (stagnant and circulated water; Fig. 6A; Table S2). The model endpoint is when the O_2 reaches the gas within the tracheal system, sub-elytral space or soft tissues. The diffusion pathway under the chitin is complicated and uncertain, because it includes soft tissue and tracheae (Fig. 2). These structures are safely ignored, because Krogh's coefficient in soft tissue is greater than 10 times higher than that in chitin (Krogh, 1919), and the tracheal walls are very thin (Fig. 2D). In circulated water, mean ΔP_{O_2} to the beetles' surface is 1.3 kPa in *P. macrosturtensis*, 0.8 kPa in *P. mesosturtensis* and 0.9 kPa in *L. palmulaoides*, which increases to 9.4, 3.8 and 6.4 kPa in stagnant water, respectively (Fig. 6A). The mean decline in P_{O_2} through the cuticle is 2.8 kPa in *P. macrosturtensis*, 1.9 kPa in *P. mesosturtensis* and 1.7 kPa in *L. palmulaoides*. In stagnant water, *P. macrosturtensis* could become O_2 limited when the aquatic P_{O_2} declines to 14.5 kPa. This assumes the P_{O_2} on the inside of the cuticle declines below an assumed critical P_{O_2} ($P_{O_2,crit}$) of 2.3 kPa, as found in the water bug *Agraptocorixa eurynome*, under which metabolism becomes limited (Matthews and Seymour, 2010). In *P. mesosturtensis*, limitation could occur at 8.0 kPa aquatic P_{O_2} and 10.4 kPa for *L. palmulaoides*. These O_2 levels are similar to the lowest values recorded at Sturt Meadows (Fig. S1). However,

Journal of Experimental Biology (2019) 222, jeb196659. doi:10.1242/jeb.196659

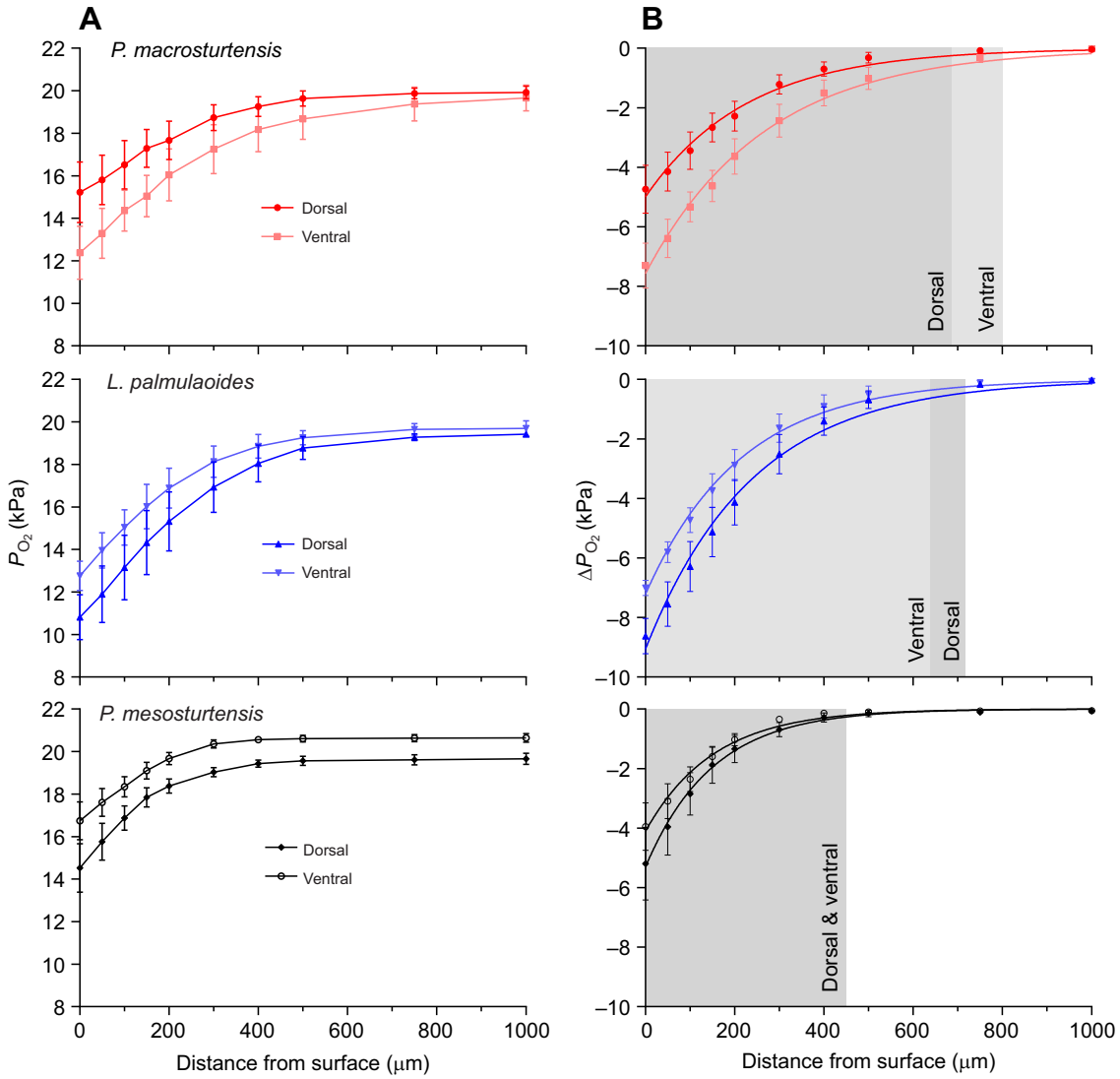

Fig. 4. O_2 boundary layers. (A) Mean P_{O_2} transects from the dorsal and ventral surfaces of *P. macrosturtensis*, *L. palmulaoides* and *P. mesosturtensis* in stagnant water. (B) Mean P_{O_2} difference between the maximum P_{O_2} recorded in a transect and the P_{O_2} at a particular distance from the beetle's surface. A one-phase association shows the approximate effective boundary layer profile in which the thickness is defined as where the ΔP_{O_2} is 5% different from 0, and 100% is the *y*-intercept (Y_0, see Materials and Methods). Six individuals of each species were used, three each for dorsal and ventral measurements, with five transects per individual. Mean water temperature during all P_{O_2} transects was 25.3±0.4°C. Shown are means and 95% CIs.

activity such as swimming or crawling, or water convection (Fig. 6Ai) would thin the boundary layer, enabling a higher metabolism without limitation under these P_{O_2} levels.

Differences between the model and experimental results arise when considering O_2 uptake per unit surface area. $\dot{M}_{O_2}$ is 36.5 pmol s^{-1} cm^{-2} in *P. macrosturtensis*, 24.6 pmol s^{-1} cm^{-2} in *P. mesosturtensis* and 26.4 pmol s^{-1} cm^{-2} in *L. palmulaoides*. These values result in a similar boundary layer thickness for *P. mesosturtensis* and *L. palmulaoides*; however, the experiments show the boundary layer is thinner in *P. mesosturtensis* (Fig. 4). The difference may be linked to the smaller size of *P. mesosturtensis*, in which diffusion is closer to radial than linear as assumed in Fick's diffusion equation for the other species. Nevertheless, despite the similarity in size, *L. palmulaoides* is likely to be more tolerant of low P_{O_2} compared with *P. macrosturtensis* because of a better ratio of surface area to $\dot{M}_{O_2}$ and a thinner cuticle (Table 1, Fig. 6A).

Table 2. Whole-animal and mass-specific O_2 consumption rates ($\dot{M}_{O_2}$) for subterranean dytiscids

Species (*N*)	Dry mass (mg)	Wet mass (mg)	Whole-animal $\dot{M}_{O_2}$ (nmol h^{-1})	Mass-specific $\dot{M}_{O_2}$ (nmol h^{-1} mg^{-1})
*P. macrosturtensis** (7)	–	2.52±0.16	26.5±3.1	10.6±1.7
P. macrosturtensis (7)	0.91±0.24	2.71±0.72	20.1±3.3	7.9±1.6
P. mesosturtensis‡ (5)	0.19±0.02	0.55±0.05	4.2±1.0	7.7±2.2
L. palmulaoides (6)	0.78±0.21	2.32±0.62	15.1±2.8	7.1±1.9

*$\dot{M}_{O_2}$ measured in air+water chambers (water temperature 25.1±0.0°C). In water-only chambers, water temperature was maintained between 24.4 and 25.6°C at the field station. Underlined wet mass values were calculated from dry mass. ‡Mean individual $\dot{M}_{O_2}$ and mass of four beetles within each chamber of *N*=5 experiments. Means and 95% CIs shown with *N* in parentheses.

Journal of Experimental Biology (2019) 222, jeb196659. doi:10.1242/jeb.196659

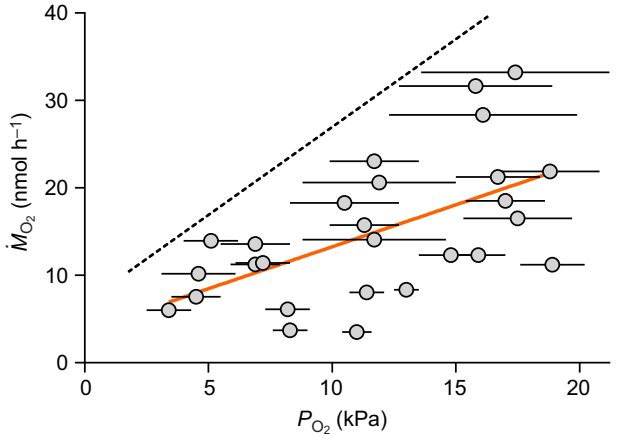

Fig. 5. O_2 consumption rate of *P. macrosturtensis* when exposed to varying initial P_{O_2} levels in the water-only chambers. Each point represents the mean P_{O_2} and O_2 consumption rate ($\dot{M}_{O_2}$) while the beetles were in the chamber for a particular experiment (N=11 individual beetles, N=27 data points). Horizontal bars represent the P_{O_2} range over which $\dot{M}_{O_2}$ was measured. A linear regression of the decline in $\dot{M}_{O_2}$ is shown by the solid orange line ($\dot{M}_{O_2}$=0.959×P_{O_2}+3.673, R^2=0.33) and the dashed line illustrates the trend of decline in the upper bounds of $\dot{M}_{O_2}$ measurements.

The model can be adjusted to make predictions about O_2 limitation with increasing beetle size. This is achieved by taking the average relationship between length, width and height of the three subterranean diving beetles and increasing the size of a hypothetical beetle (assuming a lozenge shape; Tables S1, S2 and Fig. S2). This model assumes circulated water and cuticle thickness increase with mass according to the equation determined in Fig. 3. $\dot{M}_{O_2}$ scaling began with a resting metabolic rate of 0.2 nmol h^{-1} at 0.04 mg up to 24.2 nmol h^{-1} and 4.82 mg (5 mm), which is approximately the size of the largest known subterranean dytiscid. Increments in metabolic rate up to 10-fold represent the potential metabolic scope of the beetles. There is little effect of size on the P_{O_2} at the surface of the cuticle (Fig. 6Bi). A thicker boundary layer would have a greater effect; however, given the animals would be moving when metabolic rates are high, this would not limit the system. Cuticle thickness has a greater effect on internal P_{O_2} (Fig. 6Bii). Although the estimated resting metabolism does not become limited at the maximum beetle size, the metabolic scope is reduced. A beetle such as *P. mesosturtensis* would be able to increase metabolic rate more than 10 times above resting levels; however, *P. macrosturtensis* and *L. palmulaoides* have a calculated metabolic scope of only 4–5 times resting, which is similar to the narrower metabolic scopes recorded between rest and terrestrial activity in several beetle species (Bartholomew and Casey, 1977; Rogowitz and Chappell, 2000).

Metabolic scope and oxygen availability

When *P. macrosturtensis* was exposed to declining P_{O_2}, both metabolic scope and $\dot{M}_{O_2}$ tended to decrease, as shown by the linear decline in $\dot{M}_{O_2}$ as well as a linear decline in the upper $\dot{M}_{O_2}$ values recorded (Fig. 5). Each point in Fig. 5 represents the mean $\dot{M}_{O_2}$ of the beetle while it was in the chamber. However, because the beetles' activity cannot be controlled, they may be more or less active during the experiments, producing a range of mean $\dot{M}_{O_2}$ at a given P_{O_2}. Fig. 7 shows the experimental results can be explained by varying levels of activity during each experiment, where maximum metabolic rate declines linearly with P_{O_2} and is therefore O_2 limited, but resting metabolic rate remains unaffected. Experimentally measured values below the calculated values may indicate a lower resting metabolic rate than anticipated or that resting metabolic rate is affected at lower P_{O_2}. The model results in Fig. 7 would differ if the proportion of the experiment in which the beetles were active changed or the metabolic scope changed. However, if maximum metabolic rate is O_2 limited and the beetles' activity is variable, the same general trend would occur.

A considerable reduction in metabolic scope could limit particularly larger beetles' ability to successfully occupy and utilise a subterranean habitat. Reduction in metabolic rate has been suggested as an adaptation to stressful environments, enabling a greater allocation of resources to growth, reproduction and development (Chown and Gaston, 1999). If the metabolic scope becomes narrower in larger beetles, this could also limit the resources available for growth, reproduction and development. Additionally, declines in aquatic O_2 levels reduce the beetles' metabolic scope. The largest known subterranean dytiscids, *Limbodessus magnificus* and *Limbodessus hahni* at 4.8 mm long, equivalent to 4.3 mg (Fig. 6B; Balke et al., 2004; Watts and Humphreys, 2009), may represent the upper size limit of these beetles which still have a functional metabolic scope. If small subterranean dytiscids are found to have a greater metabolic scope than larger species, this would support the idea that a reduction in metabolic scope associated with cutaneous respiration limits subterranean beetle size.

Body size, metabolic rate and cuticle thickness

The metabolic rate of subterranean dytiscids is lower than that of resting insects generally, and of plastron breathing insects (Fig. 8). In plastron breathers, their low metabolic rate is associated with the significant resistance to O_2 diffusion that the boundary layer provides (Seymour and Matthews, 2013). The subterranean beetles have, in addition to the boundary layer, resistance of the cuticle, which corresponds with a further reduced metabolism. However, there are other factors that could contribute to a lowered metabolic rate. Subterranean dytiscids have reduced wings and are unable to fly (Watts and Humphreys, 2006), and insects that undertake low-energy activities have lower resting metabolism than those that do high-energy activities like flying (Reinhold, 1999). Low metabolism has also been associated with low and variable O_2 levels in subterranean aquatic isopods and amphipods (Hervant et al., 1998; Malard and Hervant, 1999), and resource limitation in subterranean environments (Hüppop, 1985). It is unclear whether the beetles in the Sturt Meadows and Laverton aquifers are resource limited, but they are exposed to variable O_2 levels. In the Sturt Meadows aquifer, O_2 saturation ranges from ∼50% to 100% in boreholes known to have beetles (Fig. S1), and O_2 saturation can vary by more than 40% within an individual borehole. This variability within and between boreholes has also been recorded in other aquifers containing dytiscids (Watts and Humphreys, 2006).

The cuticle thickness of the three subterranean species in this study was between 6.3 and 8.4 µm, and was similar between the species despite the size differences (Table 1). These measurements give an indication of the thickness of two major surfaces of the beetles, the elytra and ventral sternites. However, cuticle thickness varies across the body, including overlap of sternites, and the edges of the elytra over the edge of the abdomen, which could influence O_2 diffusion. The similarity in cuticle thickness between the subterranean species may indicate a trade-off between being thin enough to facilitate cutaneous respiration and thick enough to provide sufficient strength and integrity to allow the beetles to function within their environment without physical damage

Journal of Experimental Biology (2019) 222, jeb196659. doi:10.1242/jeb.196659

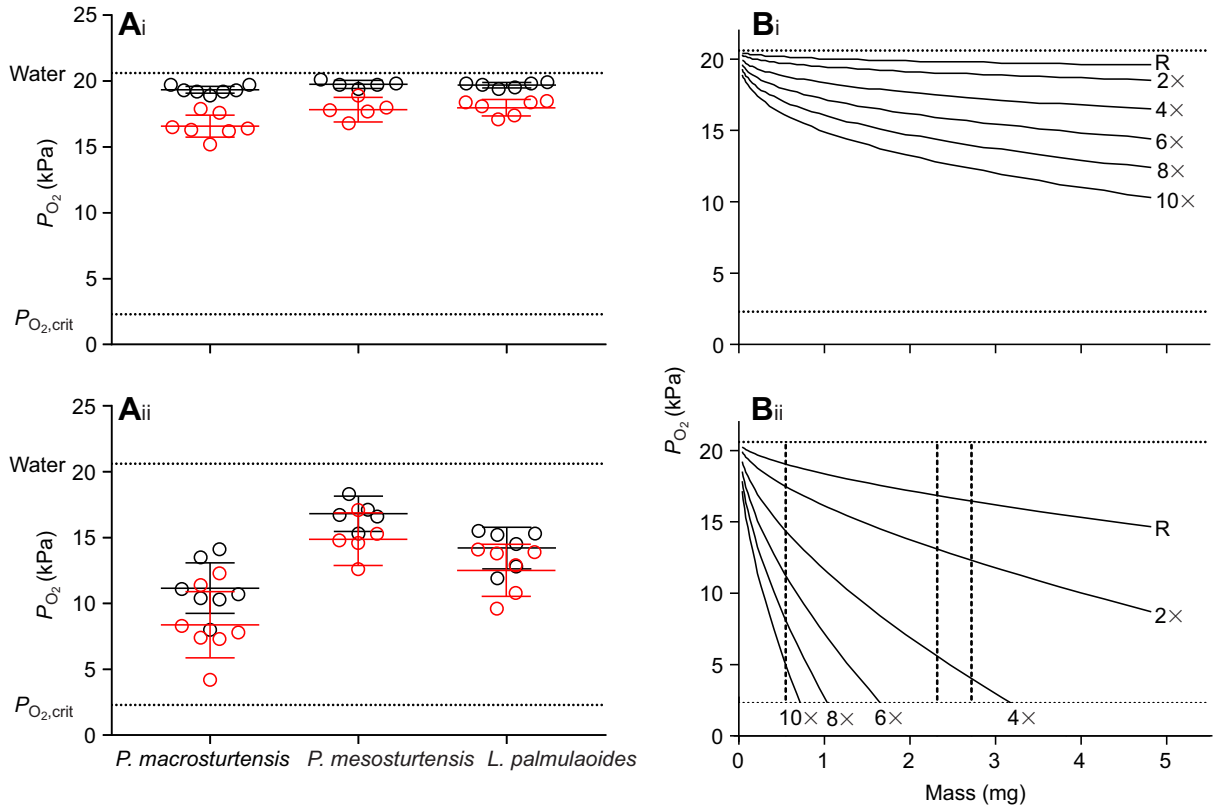

Fig. 6. Calculated P_{O_2} through the O_2 cascade of subterranean dytiscids. Data were obtained using Fick's general diffusion equation (Table S1 and S2). (A) Calculated P_{O_2} on the surface (black) of the beetles and on the inside (red) of the cuticle using the experimentally measured $\dot{M}_{O_2}$ from beetles in this study. Ai shows calculated P_{O_2} under convected conditions with 100 µm boundary layers. Aii represents stagnant water, with boundary layer thicknesses of 750 µm for *P. macrosturtensis*, 700 µm for *L. palmulaoides* and 450 µm for *P. mesosturtensis* (mean of dorsal and ventral boundary layers rounded to the nearest 50 µm). Means are shown with 95% CIs. (B) Model estimates of P_{O_2} (solid lines) at the surface (Bi) and on the inner side of the cuticle (Bii) of a generalised subterranean diving beetle with increasing size. 'R' indicates the predicted resting metabolic rate regression estimated from the lowest $\dot{M}_{O_2}$ measurements undertaken in air-equilibrated water in water-only chambers, where estimated resting $\dot{M}_{O_2}$ is 13 nmol h^{-1} in *P. macrosturtensis*, 2.5 nmol h^{-1} in *P. mesosturtensis* and 11.5 nmol h^{-1} in *L. palmulaoides* ($\dot{M}_{O_2}$=4.68$M_b^{1.04}$). Estimated resting metabolism was then multiplied by 2, 4, 6, 8 and 10, indicated at the end of each P_{O_2} line. Boundary layer thickness was 100 µm. The dashed vertical lines in Bii represent the mass of the three subterranean dytiscids used in the model. Beetle length (mm)=2.96$M_b^{0.33}$. In both A and B, the top dotted line shows the air-saturated water P_{O_2} at 25°C (20.6 kPa) and the bottom dotted line is $P_{O_2,crit}$ (2.3 kPa) the critical P_{O_2} under which the metabolism becomes limited. Krogh's coefficient for water is 0.290 pmol s^{-1} kPa^{-1} cm^{-1} (Seymour, 1994), and for cuticle it is 0.010 pmol s^{-1} kPa^{-1} cm^{-1}, adjusted to 25°C with a Q_{10} of 1.1 (Bartels, 1971; Krogh, 1919).

(Lane et al., 2017). Surface dytiscids may require thicker cuticles to resist damage from high-energy environments and to protect them from predators. This hypothesis is supported by surface species *S. clavatus* and *N. dispar* having thicker than expected cuticles given their mass (Fig. 3), and potentially why the surface dytiscid *Deronectes aubei*, which has a relatively thick cuticle given its size (~50 µm; Kehl and Dettner, 2009), uses setal tracheal gills. The tracheal gills reduce resistance to O_2 diffusion, which would be much greater through the unelaborated cuticle, while still maintaining its strength.

Cuticle thickness of the subterranean beetles is within the range of that of other cutaneously respiring insects. Fifth instar *Aphelocheirus aestivalis* (20 mg) respire through a 45 µm thick cuticle (Thorpe and Crisp, 1947b), and the diffusion distance of the tracheal gills of lestid damselfly larvae is estimated at 10–20 µm (Eriksen, 1986). In *D. aubei*, diffusion distance through the respiratory setae is <1 µm, like in the tracheal gills of Trichoptera larvae (Kehl and Dettner, 2009).

As dytiscids become larger, the internal structure of the elytra changes (Fig. 2). In the subterranean and small surface dytiscids, the elytra consists of a layer of cuticular laminae with a layer of soft tissue on the ventral surface containing the tracheae (Fig. 2D). However, in the larger dytiscids, haemolymph spaces occur within the cuticular laminae separated by pillar-like trabeculae (Fig. 2A–C). The spaces may help lighten the elytra, assisting with flight, and the trabeculae provide additional mechanical strength (Ni et al., 2001; Van de Kamp and Greven, 2010). The tracheae, which appear to be within the haemolymph spaces (Iwamoto et al., 2002), would allow diffusion of respiratory gases throughout the elytra. This may also allow O_2 diffusion into the tracheal system through the cuticle from the water, or from the sub-elytral cavity, the latter being more likely because of the ventral cuticular laminae being thinner than the dorsal cuticular laminae. Some beetles have air sacs within the elytra (Chen and Wu, 2013; Gokan, 1966); however, it is unclear whether they are present in the larger dytiscids.

The subterranean beetles in this study differ from surface dytiscids that use air stores and gas gills and return to the surface regularly. However, they also differ from submergence-tolerant surface dytiscids because they lack structures like respiratory setae or pores (Fig. 1). The submergence-tolerant dytiscid *D. aubei* have ~20 µm long, spoon-shaped setae on their body, which have tracheoles running to the base and probably into the setae themselves (Kehl and Dettner, 2009). These setae, which are found at a density of 5900 mm^{-2} on the elytra, allow O_2 diffusion

Journal of Experimental Biology (2019) 222, jeb196659. doi:10.1242/jeb.196659

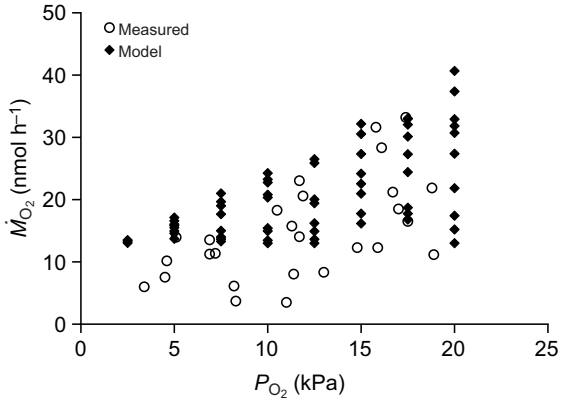

Fig. 7. Measured $\dot{M}_{O_2}$ of *P. macrosturtensis* at different P_{O_2} values compared with a model calculating $\dot{M}_{O_2}$ with differing proportions of activity during each experiment (filled diamonds). The measured values are from Fig. 5. The model parameters are that resting $\dot{M}_{O_2}$ is 13 nmol h^{-1}, comparable to the lowest values recorded for *P. macrosturtensis* in the water-only experiments, which is independent of P_{O_2} between 2.5 and 20 kPa. Maximum metabolic rate is assumed to be 10 times higher at 130 nmol h^{-1}, the metabolic scope observed in other aquatic insects (Seymour et al., 2015). This value declines linearly from 20 kPa P_{O_2} to the resting $\dot{M}_{O_2}$ at 2.5 kPa, representing diffusion limitation at maximum metabolic rate. Each model point signifies the mean $\dot{M}_{O_2}$ given a randomly selected proportion between 0 and 0.25 of the experiment that a beetle is active and at the maximum metabolic rate, with the remainder of the time spent at resting $\dot{M}_{O_2}$. Therefore, $\dot{M}_{O_2}$=$\dot{M}_{O_2,max}$ at a given P_{O_2}×proportion of time active+resting $\dot{M}_{O_2}$×proportion of time inactive. At each P_{O_2} (20, 17.5, 15, 12.5, 10, 7.5, 5 and 2.5 kPa), 10 model iterations are shown.

from the water into the tracheal system through the thin cuticle of the setae (<1 µm) traversing the ∼50 µm thick elytral cuticle (Kehl and Dettner, 2009). In other submergence-tolerant surface dytiscids, punctures, small openings in the cuticle surface from which structures emerge (Wolfe and Zimmerman, 1984), and other small openings have been identified as potentially having respiratory roles. Individual punctures or openings/pores are 7–43 µm^2 at a density of 3400–14,000 mm^{-2}. Similar structures of this size and density are absent on the subterranean dytiscid species (Fig. 1).

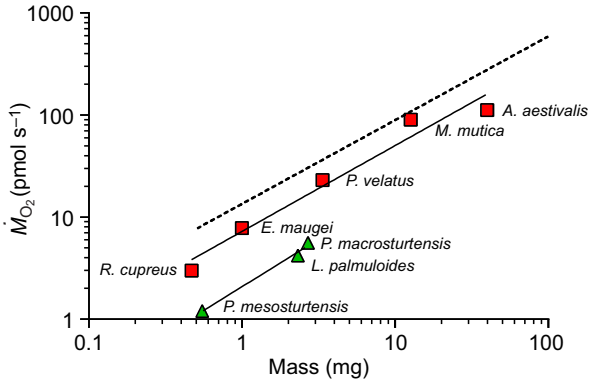

Fig. 8. Comparison of $\dot{M}_{O_2}$ and body mass in insects. The allometric analysis includes the three subterranean dytiscids from this study (triangles, $\dot{M}_{O_2}$=2.0744$M_b^{0.93}$), plastron breathing insects (Seymour and Matthews, 2013) (squares, $\dot{M}_{O_2}$=7.221$M_b^{0.84}$, adjusted to 25°C assuming a Q_{10} of 2; Chown et al., 2007) and 391 insect species (resting $\dot{M}_{O_2}$, dashed line, $\dot{M}_{O_2}$=13.452$M_b^{0.82}$) (Chown et al., 2007). The slope of the regression for plastron breathing insects is not significantly different from that for the subterranean dytiscids; however, the elevation is significantly higher (ANCOVA, P<0.05). $\dot{M}_{O_2}$ data for subterranean dytiscids are from the water-only chambers using calculated wet mass.

Ecology and evolution

Observations with the borescope in boreholes show there were more occurrences of beetles near the water's surface. This may be associated with a higher P_{O_2} near the water's surface as a result of O_2 diffusion from the atmosphere, a general trend shown in boreholes known to have beetles (Fig. S1). However, O_2 levels can be inverted within a borehole, with higher O_2 levels being deeper down (Watts and Humphreys, 2006). Beetles may also be congregating near the water's surface because insects and detritus fall into the water, providing a food source. On two occasions in the laboratory, *P. macrosturtensis* was observed to temporarily crawl out of the water completely, associated with a strong odour above the water. This behaviour is likely to be secretion grooming, which surface dytiscids undertake to reduce bacterial growth with antimicrobial chemicals and to increase wettability of the cuticle (Dettner, 1985). It may also result in the beetles being closer to the surface. Whether smaller species like *P. mesosturtensis* undertake this behaviour is unclear as they easily become stuck to the meniscus and are unable to dive. However, maintaining a clean cuticle would be important for ensuring optimal cutaneous respiration by reducing O_2 consumption caused by microbial growth, and encouraging convection of the boundary layer.

Most subterranean dytiscids are from the subfamily Hydroporinae in which members are generally <5 mm long and weigh <5 mg (Miller and Bergsten, 2016). Small size is useful for both evolving cutaneous respiration and occupying intermediate habitats between terrestrial and subterranean environments where beetles inhabit small interstitial spaces. These include water-filled gravel where surface water interfaces with ground water or where surface water dries up and ground water is used as a refuge (Kato et al., 2010; Leys et al., 2010; Leys and Watts, 2008). Other groups of dytiscids are likely not to have made the transition to the subterranean habitats because of difficulties of fitting into small spaces, limited resource availability for larger species and propensity to disperse under adverse conditions (Leys and Watts, 2008). Many aquatic insects and in particular small species are likely to benefit to some degree from cutaneous respiration (Vlasblom, 1970). The ability of these subterranean dytiscids to rely solely on this mode of respiration and at relatively high temperature has enabled this group to adapt to and survive in the aquifer environment. Given the considerable number of independent incursions into the subterranean environment (Cooper et al., 2002; Leys et al., 2003), cutaneous respiration in these dytiscids has contributed to the largest radiation of subterranean diving beetles in the world (Balke et al., 2004).

Acknowledgements

We thank Flora, Peter and Paul Axford for providing access and accommodation at the Sturt Meadows pastoral property, Chris Watts from the South Australian Museum for assisting with species identification, Lyn Waterhouse and Lisa O'Donovan from Adelaide Microscopy, William Humphreys from the Western Australian Museum for water quality data, Sally Maxwell and Silvia Clarke from DEWNR and Thomas Nelson and Qiaohui Hu from Adelaide University for assisting with collecting beetles and maintaining them, and two anonymous reviewers whose comments and suggestions helped improve this manuscript.

Competing interests

The authors declare no competing or financial interests.

Author contributions

Conceptualization: S.J.B.C., R.S.S.; Methodology: K.K.J., R.S.S.; Formal analysis: K.K.J.; Investigation: K.K.J., S.J.B.C., R.S.S.; Writing - original draft: K.K.J.; Writing - review & editing: K.K.J., S.J.B.C., R.S.S.; Visualization: K.K.J.; Supervision: S.J.B.C., R.S.S.; Project administration: K.K.J., S.J.B.C., R.S.S.; Funding acquisition: K.K.J., S.J.B.C.

Funding
K.K.J. was supported by the University of Adelaide for award of an Australian Government Research Training Program Scholarship. Funding was also provided by a Royal Society of South Australia Small Research grant to K.K.J. and an Australian Research Council Discovery grant (no. 120102132) to S.J.B.C.

Supplementary information
Supplementary information available online at
http://jeb.biologists.org/lookup/doi/10.1242/jeb.196659.supplemental

References

Balke, M., Watts, C. H. S., Cooper, S. J. B., Humphreys, W. F. and Vogler, A. P. (2004). A highly modified stygobiont diving beetle of the genus *Copelatus* (Coleoptera, Dytiscidae): taxonomy and cladistic analysis based on mitochondrial DNA sequences. *Syst. Entomol.* **29**, 59-67.
Bartels, H. (1971). Diffusion coefficients and Krogh's diffusion constants. In *Respiration and Circulation* (ed. P. L. Altman and D. S. Dittmer), pp. 21-22. Bethesda, Maryland, USA: Federation of American Societies for Experimental Biology.
Bartholomew, G. A. and Casey, T. M. (1977). Body temperature and oxygen consumption during rest and activity in relation to body size in some tropical beetles. *J. Therm. Biol.* **2**, 173-176.
Bäumer, C., Pirow, R. and Paul, R. J. (2000). Respiratory adaptations to running-water microhabitats in mayfly larvae *Epeorus sylvicola* and *Ecdyonurus torrentis*, Ephemeroptera. *Physiol. Biochem. Zool.* **73**, 77-85.
Blomberg, S. P., Garland, T. and Ives, A. R. (2003). Testing for phylogenetic signal in comparative data: behavioral traits are more labile. *Evolution* **57**, 717-745.
Calosi, P., Bilton, D. T. and Spicer, J. I. (2007). The diving response of a diving beetle: effects of temperature and acidification*. *J. Zool.* **273**, 289-297.
Chen, J. and Wu, G. (2013). Beetle forewings: epitome of the optimal design for lightweight composite materials. *Carbohydr. Polym.* **91**, 659-665.
Chown, S. L. and Gaston, K. J. (1999). Exploring links between physiology and ecology at macro-scales: the role of respiratory metabolism in insects. *Biol. Rev.* **74**, 87-120.
Chown, S. L., Marais, E., Terblanche, J. S., Klok, C. J., Lighton, J. R. B. and Blackburn, T. M. (2007). Scaling of insect metabolic rate is inconsistent with the nutrient supply network model. *Funct. Ecol.* **21**, 282-290.
Cooper, S. J. B., Hinze, S., Leys, R., Watts, C. H. S. and Humphreys, W. F. (2002). Islands under the desert: molecular systematics and evolutionary origins of stygobitic water beetles (Coleoptera: Dytiscidae) from central Western Australia. *Invertebrate Systematics* **16**, 589-598.
Dejours, P. (1981). *Principles of Comparative Respiratory Physiology*. Amsterdam, Netherlands: Elsevier/North-Holland Biomedical Press.
Dettner, K. (1985). Ecological and phylogenetic significance of defensive compounds from pygidial glands of Hydradephaga (Coleoptera). *Proc. Acad. Nat. Sci. Phila.* **137**, 156-171.
Ege, R. (1915). On the respiratory function of the air stores carried by some aquatic insects (Corixidae, Dytiscidae and Notonecta). *Zeitschrift für Allgemeine Physiologie* **17**, 81-124.
Eriksen, C. H. (1986). Respiratory roles of caudal lamellae (gills) in a lestid damselfly (Odonata:Zygoptera). *J. North. Am. Benthol. Soc.* **5**, 16-27.
Foottit, R. G. and Adler, P. H. (2009). *Insect Biodiversity: Science and Society*. Oxford, UK: John Wiley & Sons.
Gokan, N. (1966). On the tracheation and distribution of the air sacs in elytra of scarabaeid beetles. *Memoirs of the Tokyo University of Agriculture* **10**, 56-63.
Guzik, M. T., Cooper, S. J. B., Humphreys, W. F. and Austin, A. D. (2009). Fine-scale comparative phylogeography of a sympatric sister species triplet of subterranean diving beetles from a single calcrete aquifer in Western Australia. *Mol. Ecol.* **18**, 3683-3698.
Guzik, M. T., Cooper, S. J. B., Humphreys, W. F., Ong, S., Kawakami, T. and Austin, A. D. (2011). Evidence for population fragmentation within a subterranean aquatic habitat in the Western Australian desert. *Heredity* **107**, 215-230.
Hervant, F., Mathieu, J. and Messana, G. (1998). Oxygen consumption and ventilation in declining oxygen tension and posthypoxic recovery in epigean and hypogean crustaceans. *J. Crustac. Biol.* **18**, 717-727.
Hüppop, K. (1985). The role of metabolism in the evolution of cave animals. *The NSS Bulletin* **47**, 136-146.
Hutchinson, G. E. (1981). Thoughts on aquatic insects. *Bioscience* **31**, 495-500.
Iwamoto, M., Chen, J., Kurashiki, K. and Ni, Q.-Q. (2002). Chitin fibre and its laminated structure of the fore-wing of beetle. *WIT Transactions on The Built Environment* **59**, 127-136.
Jones, K. K., Snelling, E. P., Watson, A. P. and Seymour, R. S. (2015). Gas exchange and dive characteristics of the free-swimming backswimmer *Anisops deanei*. *J. Exp. Biol.* **218**, 3478-3486.
Jones, K. K., Hetz, S. K. and Seymour, R. S. (2018). The effects of temperature, activity and convection on the plastron PO_2 of the aquatic bug *Aphelocheirus aestivalis* (Hemiptera; Aphelocheiridae). *J. Insect Physiol.* **106**, 155-162.
Kato, M., Kawakita, A. and Kato, T. (2010). Colonization to aquifers and adaptations to subterranean interstitial life by a water beetle clade (Noteridae) with description of a new *Phreatodytes* species. *Zoolog. Sci.* **27**, 717-722.
Kehl, S. (2014). Respiration and Tracheal System. In *Ecology, Systematics, and the Natural History of Predaceous Diving Beetles* (*Coleoptera: Dytiscidae*), (ed. D. A. Yee), pp. 189 - 198. Dordrecht, Netherlands: Springer.
Kehl, S. and Dettner, K. (2009). Surviving submerged—Setal tracheal gills for gas exchange in adult rheophilic diving beetles. *J. Morphol.* **270**, 1348-1355.
Krogh, A. (1919). The rate of diffusion of gases through animal tissues, with some remarks on the coefficient of invasion. *J. Physiol.* **52**, 391-408.
Lane, S. J., Shishido, C. M., Moran, A. L., Tobalske, B. W., Arango, C. P. and Woods, H. A. (2017). Upper limits to body size imposed by respiratory–structural trade-offs in Antarctic pycnogonids. *Proc. R. Soc. B* **284**, 20171779.
Leijs, R., van Nes, E. H., Watts, C. H. S., Cooper, S. J. B., Humphreys, W. F. and Hogendoorn, K. (2012). Evolution of blind beetles in isolated aquifers: a test of alternative modes of speciation. *PLoS One* **7**, e34260.
Leys, R. and Watts, C. H. S. (2008). Systematics and evolution of the Australian subterranean hydroporine diving beetles (Dytiscidae), with notes on *Carabhydrus*. *Invertebrate Systematics* **22**, 217-225.
Leys, R., Watts, C. H. S., Cooper, S. J. B. and Humphreys, W. F. (2003). Evolution of subterranean diving beetles (Coleoptera: Dytiscidae: Hydroporini, Bidessini) in the arid zone of Australia. *Evolution* **57**, 2819-2834.
Leys, R., Roudnew, B. and Watts, C. H. S. (2010). *Paroster extraordinarius* sp. nov., a new groundwater diving beetle from the Flinders Ranges, with notes on other diving beetles from gravels in South Australia (Coleoptera: Dytiscidae). *Aust. J. Entomol.* **49**, 66-72.
Madsen, B. L. (2012). Submersion respiration in small diving beetles (Dytiscidae). *Aquat. Insects* **34**, 57-76.
Malard, F. and Hervant, F. (1999). Oxygen supply and the adaptations of animals in groundwater. *Freshw. Biol.* **41**, 1-30.
Marx, M. T. and Messner, B. (2012). A general definition of the term "plastron" in terrestrial and aquatic arthropods. *Organisms Diversity and Evolution* **12**, 403-408.
Matthews, P. G. D. and Seymour, R. S. (2010). Compressible gas gills of diving insects: measurements and models. *J. Insect Physiol.* **56**, 470-479.
Miller, K. B. and Bergsten, J. (2016). *Diving Beetles of the World: Systematics and Biology of the Dytiscidae*. Baltimore, Maryland, USA: JHU Press.
Morgan, A. H. and O'Neil, H. D. (1931). The function of the tracheal gills in larvae of the caddis fly, Macronema zebratum Hagen. *Physiol. Zool.* **4**, 361-379.
Mueller, C. A. and Seymour, R. S. (2011). The importance of perivitelline fluid convection to oxygen uptake of *Pseudophryne bibronii* eggs. *Physiological and Biochemical Zoology: Ecological and Evolutionary Approaches* **84**, 299-305.
Ni, Q.-Q., Chen, J., Iwamoto, M., Kurashiki, K. and Saito, K. (2001). Interlaminar reinforcement mechanism in a beetle fore-wing. *JSME International Journal Series C Mechanical Systems, Machine Elements and Manufacturing* **44**, 1111-1116.
Noh, M. Y., Muthukrishnan, S., Kramer, K. J. and Arakane, Y. (2016). Cuticle formation and pigmentation in beetles. *Current Opinion in Insect Science* **17**, 1-9.
Ordish, R. G. (1976). Two new genera and species of subterranean water beetle from New Zealand (Coleoptera: Dytiscidae). *N. Z. J. Zool.* **3**, 1-10.
Pritchard, G., McKee, M. H., Pike, E. M., Scrimgeour, G. J. and Zloty, J. (1993). Did the first insects live in water or in air? *Biol. J. Linn. Soc.* **49**, 31-44.
Rahn, H. and Paganelli, C. V. (1968). Gas exchange in gas gills of diving insects. *Respiration Physiology* **5**, 145-164.
Rasmussen, A. (1996). Least oxygen dependent. In *University of Florida Book of Insect Records* (ed. T. J. Walker), pp. 46-48. Florida, USA: University of Florida Gainesville.
Reinhold, K. (1999). Energetically costly behaviour and the evolution of resting metabolic rate in insects. *Funct. Ecol.* **13**, 217-224.
Rogowitz, G. L. and Chappell, M. A. (2000). Energy metabolism of eucalyptus-boring beetles at rest and during locomotion: gender makes a difference. *J. Exp. Biol.* **203**, 1131-1139.
Seymour, R. S. (1994). Oxygen diffusion through the jelly capsules of amphibian eggs. *Isr. J. Zool.* **40**, 493-506.
Seymour, R. S. and Matthews, P. G. D. (2013). Physical gills in diving insects and spiders: theory and experiment. *J. Exp. Biol.* **216**, 164-170.
Seymour, R. S. and Roberts, J. D. (1995). Oxygen uptake by the aquatic eggs of the Australian frog *Crinia georgiana*. *Physiol. Zool.* **68**, 206-222.
Seymour, R. S., Jones, K. K. and Hetz, S. K. (2015). Respiratory function of the plastron in the aquatic bug *Aphelocheirus aestivalis* (Hemiptera, Aphelocheiridae). *J. Exp. Biol.* **218**, 2840-2846.
Smrž, J. (1981). Respiration – a new function of some hydroporine elytra (Coleoptera, Dytiscidae, Hydroporinae). *Acta Entomol. Bohemoslov.* **78**, 209-215.
Snelling, E. P., Duncker, R., Jones, K. K., Fagan-Jeffries, E. P. and Seymour, R. S. (2017). Flight metabolic rate of *Locusta migratoria* in relation to oxygen partial pressure in atmospheres of varying diffusivity and density. *J. Exp. Biol.* **220**, 4432-4439.
Thorpe, W. H. and Crisp, D. J. (1947a). Studies on plastron respiration I. The biology of *Aphelocheirus* [Hemiptera, Aphelocheiridae (Naucoridae)] and the mechanism of plastron retention. *J. Exp. Biol.* **24**, 227-269.
Thorpe, W. H. and Crisp, D. J. (1947b). Studies on plastron respiration II. The respiratory efficiency of the plastron in *Aphelocheirus*. *J. Exp. Biol.* **24**, 270-303.

Ueno, S. I. (1957). Blind aquatic beetles of Japan, with some accounts of the fauna of Japanese subterranean waters. *Archiv für Hydrobiologie* **53**, 250-296.
Van de Kamp, T. and Greven, H. (2010). On the architecture of beetle elytra. *Entomologie heute* **22**, 191-204.
Verberk, W. C. E. P., Calosi, P., Spicer, J. I., Kehl, S. and Bilton, D. T. (2018). Does plasticity in thermal tolerance trade off with inherent tolerance? The influence of setal tracheal gills on thermal tolerance and its plasticity in a group of European diving beetles. *J. Insect Physiol.* **106**, 163-171.
Vlasblom, A. G. (1970). The respiratory significance of the physical gill in some adult insects. *Comp. Biochem. Physiol.* **36**, 377-385.
Watts, C. H. S. and Hamom, H. (2014). *Pictorial Guide to the Diving Bettles (Dytiscidae) of South Australia*. Adelaide, South Australia, Australia: Entomology Department South Australian Museum.
Watts, C. H. S. and Humphreys, W. F. (2006). Twenty-six new Dytiscidae (Coleoptera) of the genera *Limbodessus* Guignot and *Nirripirti* Watts & Humphreys, from underground waters in Australia. *Trans. R. Soc. S. Aust.* **130**, 123-185.
Watts, C. H. S. and Humphreys, W. F. (2009). Fourteen new Dytiscidae (Coleoptera) of the genera *Limbodessus* Guignot, *Paroster* Sharp, and *Exocelina* Broun from underground waters in Australia. *Trans. R. Soc. S. Aust.* **133**, 62-107.
Wichard, W. and Komnick, H. (1974). Structure and function of the respiratory epithelium in the tracheal gills of stonefly larvae. *J. Insect Physiol.* **20**, 2397-2406.
Wolfe, G. W. and Zimmerman, J. R. (1984). Sensilla, punctation, reticulation, and body shape in the Hydroporinae (Coleoptera: Dytiscidae). *Int. J. Insect Morphol. Embryol.* **13**, 373-387.
Zar, J. H. (1998). *Biostatistical Analysis*. Englewood Cliffs, NJ, USA: Prentice-Hall.

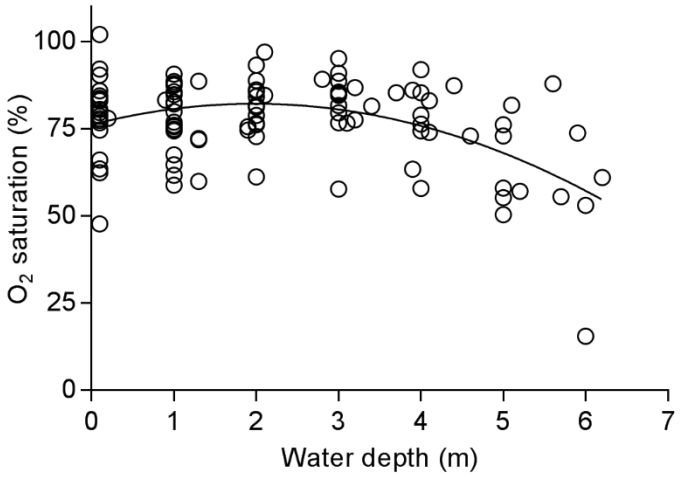

Figure S1. Change in O_2 saturation with depth in boreholes known to have subterranean beetles at the Sturt Meadows aquifer (*N*=22 boreholes, *N*=107 samples). Second order polynomial regression, $y = 76.11+6.079x+-1.539x^2$. Data collected April 2015, courtesy William (Bill) Humphreys, Western Australian Museum.

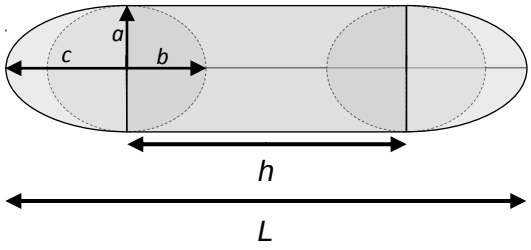

Figure S2. 3D geometric lozenge shape model that approximates the shape of subterranean diving beetles and allows estimation of surface area of the beetle. Axis a<*b, b*=*c*, *L* = total length, and h = elliptical cylinder length (*L* – 2*c*). Axis b is perpendicular to the plane of the page.

References

Bartels, H. (1971). Diffusion coefficients and Krogh's diffusion constants. In *Respiration and Circulation*, eds. P. L. Altman and D. S. Dittmer), pp. 21-22. Bethesda, Maryland, USA: Federation of American Societies for Experimental Biology.

Dejours, P. (1981). Principles of comparative respiratory physiology. Amsterdam, Netherlands: Elsevier/North-Holland Biomedical Press.

Krogh, A. (1919). The rate of diffusion of gases through animal tissues, with some remarks on the coefficient of invasion. *The Journal of Physiology* **52**, 391-408.

Matthews, P. G. D. and Seymour, R. S. (2008). Haemoglobin as a buoyancy regulator and oxygen supply in the backswimmer (Notonectidae, *Anisops*). *Journal of Experimental Biology* **211**, 3790-3799.

Rahn, H. and Paganelli, C. V. (1968). Gas exchange in gas gills of diving insects. *Respiration Physiology* **5**, 145-164.

Seymour, R. S. (1994). Oxygen diffusion through the jelly capsules of amphibian eggs. *Israel Journal of Zoology* **40**, 493-506.

Seymour, R. S., Jones, K. K. and Hetz, S. K. (2015). Respiratory function of the plastron in the aquatic bug *Aphelocheirus aestivalis* (Hemiptera, Aphelocheiridae). *Journal of Experimental Biology* **218**, 2840-2846.

Spiegel, M. R., Lipschutz, S. and Liu, J. (2013). Mathematical handbook of formulas and tables. USA: The McGraw-Hill Companies, Inc.

Watts, C. H. S. and Humphreys, W. F. (2006). Twenty-six new Dytiscidae (Coleoptera) of the genera *Limbodessus* Guignot and *Nirripirti* Watts & Humphreys, from underground waters in Australia. *Transactions of the Royal Society of South Australia* **130**, 123-185.

Table S1. A mathematical model based on Fick's general diffusion equation to calculate P_{O_2} at different points within the O_2 cascade of subterranean diving beetles to determine where limitations to cutaneous respiration may exist. The model calculates the P_{O_2} at the surface of the beetle and on the inside of the cuticle representing O_2 diffusion through the boundary layer and cuticle, respectively. The model has the following assumptions: (1) surface area for gas exchange (A) is defined as the surface area of a lozenge (ellipsoid and elliptical cylinder, Fig. S2), (2) conductance of O_2 is constant through the water or cuticle and is the product of the Krogh's coefficient of O_2 in each medium and the quotient of A and boundary layer (X_w) or cuticle thickness (X_c), (3) water is well-mixed and in equilibrium with atmospheric P_{O_2} (20.6 kPa) at 25°C, and (4) diffusion to and into the surface of the beetle is linear. Variables and constants used in the model are shown in Table S2, and O_2 consumption rate values are those measured experimentally in the water-only chambers (Table 2).

Equation		*Description*
(1)	$\dot{M}_{O_2} = K_{O_2} \times A/X \times \Delta P_{O_2}$	Fick's diffusion equation used to describe O_2 diffusion through water to a respiratory surface (Rahn and Paganelli, 1968). Where $\dot{M}_{O_2}$ (pmol s^{-1}) is the rate of O_2 consumption, K_{O_2} (pmol s^{-1} kPa^{-1} cm^{-1}) is the Krogh's coefficient of diffusion, the product of capacitance and diffusivity, A (cm^2) is the surface area for gas exchange, X (cm) is the boundary layer thickness, a fluid layer above a respiratory surface deficient in O_2 that provides resistance to O_2 diffusion, and ΔP_{O_2} (kPa) is the P_{O_2} difference between the surrounding water and respiratory surface.
(2)	$P_{O_{2,s}} = P_{O_{2,w}} - ((\dot{M}_{O_2} \times X_w)/(K_{O_{2,w}} \times A))$	Rearrangements of Eq. 1 allow the calculation of P_{O_2} at the surface of the beetle (Eq. 2, $P_{O_{2,s}}$, kPa) and on the inside of the cuticle (Eq. 3, $P_{O_{2,in}}$, kPa), representing diffusion through the boundary layer and cuticle respectively. Where $P_{O_{2,w}}$, is the P_{O_2} of the bulk surrounding water, $\dot{M}_{O_2}$ is the experimentally determined O_2 consumption rate, X_w is the O_2 boundary layer surrounding the surface of the beetle, X_c is the cuticle thickness, $K_{O_{2,w}}$ is the Krogh's coefficient for water, $K_{O_{2,C}}$ is the Krogh's coefficient for the cuticle, and A is the surface area for gas exchange.
(3)	$P_{O_{2,in}} = P_{O_{2,s}} - ((\dot{M}_{O_2} \times X_c)/(K_{O_{2,c}} \times A))$	

(4)	$A = 4\pi((ab)^{1.6}+(ac)^{1.6}+(bc)^{1.6}) \div 3)^{1/1.6} + (2\pi\sqrt{(1/2(a^2 + b^2))} \times h)$	Surface area of the beetle (*A*) can be calculated assuming the beetles are a lozenge shape, the sum of an ellipsoid (Knud-Thomsen approximation, the two ends) and an elliptical cylinder (the middle) (Michon, 2015 [http://www.numericana.com/answer/ellipsoid.htm#thomsen]; Spiegel et al., 2013), according to Eq. 4. Semi-axes *a*, *b* and *c*, and length (*h*) of the elliptical cylinder are shown in Fig. S2. Axis *b* (half of beetle width) is determined for each species from the diagrams given in Watts and Humphreys (2006), with the total length to width ratio (*L*:2*b*) being 1:2.5 for *P. macrosturtensis*, 1:2.97 for *L. palmulaoides*, and 1:2.45 for *P. mesosturtensis*. Axis *c* equals axis *b*. Axis *a* is determined for each species in the model by producing a linear regression of the mass of the lozenge, where mass (mg) $M_b = V \times 1078.4$ mg cm^{-3} (Density value determined for backswimmers, (Matthews and Seymour, 2008)) with an increasing value for *a*. Volume (*V*, cm^3) is determined with Eq. 5, the sum of the volume of an ellipsoid and elliptical cylinder (Spiegel et al., 2013). The linear mass regression is then rearranged to calculate *a* from the predicted wet mass of each species. The model can be adjusted to calculate P_{O_2} with increasing size by taking the average ratios between *L* and axes *a*, *b* and *c* (*a* = 1:10.3, *b*,*c* = 1:5.3) in the three beetle species and maintaining the ratios of axes with increasing length. The size range used was 0.04 – 4.82 mg (*L* = 0.1 – 5 mm).
(5)	$V = 4/3\pi abc + \pi abh$	Calculation for the volume of the lozenge shape.

Journal of Experimental Biology • Supplementary information

Table S2. Variables and constants used in the mathematical model to calculate the P_{O_2} at the surface of the beetle and on the inside of the cuticle (Table S1).

Variable	Value	Units	Reference
$P_{O_{2,W}}$	20.6	kPa	1
X_w	0.010 (circulated water, all species), 0.075 (*P. macrosturtensis* in stagnant water), 0.070 (*L. palmulaoides* in stagnant water), 0.045 (*P. mesosturtensis* in stagnant water)	cm	2, 3
X_c	0.00076 *P. macrosturtensis*, 0.00078 *P. mesosturtensis*, 0.000645 *L. palmulaoides*	cm	3
$K_{O_{2,W}}$	0.290	pmol s^{-1} kPa^{-1} cm^{-1}	4
$K_{O_{2,C}}$	0.010	pmol s^{-1} kPa^{-1} cm^{-1}	5, 6
a	0.042 *P. macrosturtensis*, 0.027 *P. mesosturtensis*, 0.032 *L. palmulaoides*	cm	3
b, *c*	0.08 *P. macrosturtensis*, 0.039 *P. mesosturtensis*, 0.086 *L. palmulaoides*	cm	3, 7
L	0.4 *P. macrosturtensis*, 0.23 *P. mesosturtensis*, 0.42 *L. palmulaoides*	cm	7
Mb	2.72 *P. macrosturtensis*, 0.55 *P. mesosturtensis*, 2.32 *L. palmulaoides*	mg	3

References: 1, Dejours, 1981; 2, Seymour *et al.*, 2015; 3, present study; 4, Seymour, 1994; 5, Krogh, 1919; 6, Bartels, 1971; 7, Watts and Humphreys, 2006; Symbols: X_w = O_2 boundary layer thickness, X_c = cuticle thickness, $K_{O_{2,W}}$ = Krogh's coefficient of diffusion for O_2 in water at 25°C, $K_{O_{2,C}}$ = Krogh's coefficient for chitin used for the cuticle, adjusted to 25°C with a Q_{10} of 1.1 according to Bartels (1971) , *a* = semi-axis *a* of the lozenge shape used to estimate surface area of the beetles, *b* = semi-axis *b* of lozenge, *c* = semi-axis *c* of lozenge shape, *L* = total length of lozenge shape, and total length of each beetle species (See Fig. S2), Mb = beetle body mass.